ChemPubSoc Europe

CHEMISTRY
A European Journal
Full Paper

Remote Catalyst Tuning

Improving Catalyst Activity in Hydrocarbon Functionalization by Remote Pyrene-Graphene Stacking

Pilar Ballestin,[a] David Ventura-Espinosa,[b] Santiago Martín,[c] Ana Caballero,*[a] Jose A. Mata*[b] and Pedro J. Pérez*[a]

Abstract: A copper complex bearing an N-heterocyclic carbene ligand with a pyrene-tail attached to the backbone has been prepared and supported onto reduced graphene oxide (rGO). Both copper materials have been employed as homogeneous and heterogeneous catalysts in the functionalization of hydrocarbons such as hexane, cyclohexane and benzene upon incorporation of the $CHCO_2Et$ unit from ethyl diazoacetate. The graphene-anchored complex displays higher reaction rates and induces higher yields than its soluble counterpart, features which can be explained as the result of a decrease of electron density at the metal center due to a remote net electronic flux from the supported copper complex to the graphene surface through the pyrene tag.

Introduction

The outstanding development of homogeneous catalysis in the last half-century has provided a plethora of novel transformations[1] albeit very few have reached the use at the industrial level. One of the main drawbacks toward that end stands on the operations derived from catalyst separation and further recycling, which is of particular interest when using precious metals.[2] Because of this, the strategy of anchoring tested homogeneous catalysts onto supports that would facilitate such operations is gaining importance in this homogeneous-to-heterogeneous frontier. [3] Two main factors must be considered for the success of this transition: (ii) the catalyst activity in terms of reaction kinetics and (ii) the selectivity of the transformation. Ideally, the fixation of the catalyst on a solid support should proceed without any alteration of the previous features. Also the catalytic pocket must remain unaltered, the lack of interactions between the latter and the support being crucial to ensure that the catalytic reaction in the homogeneous phase also occurs in the heterogeneous counterpart in the same manner.

One of our groups has been working in the last decades in the field of alkane C-H bond catalytic functionalization by carbene insertion, using diazo compounds as the carbene source (Scheme 1). [4] The appropriate election of the catalyst, usually a group 11 metal complex bearing a trispyrazolylborate or an NHC ligand, allowed the conversion of unreactive C-H bonds of linear, branched or cyclic alkanes, even those of methane or ethane. [5] To promote catalyst separation and recycling, we have previously developed this transformation under biphasic conditions[6] or using modified silica[7] as the support for tethered catalysts, in both cases the catalyst performance being similar when compared with the corresponding homogenous system. Following this research program, we have now turned our attention into graphene materials as solid supports for catalyst bearing polyaromatic fragments, a well-known antenna that promotes strong aromatic π–π stacking and therefore fixation on the

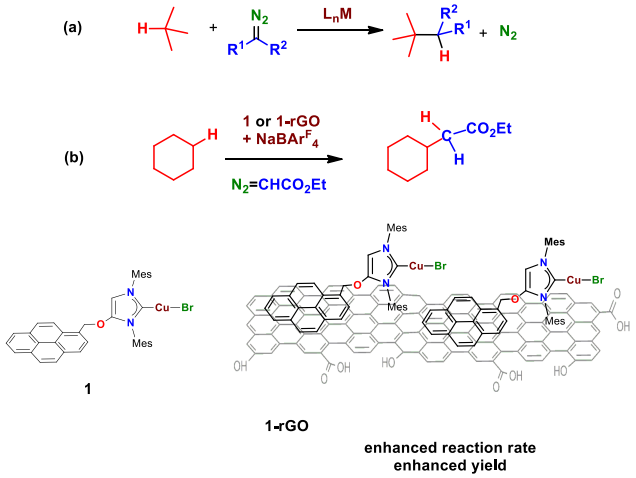

Scheme 1. (a) The metal-catalyzed functionalization of C-H bonds through carbene insertions from diazo compounds. (b) This work. The benchmarking reaction of cyclohexane with ethyl diazoacetate catalysed by complex **1** or supported **1** in reduced graphene oxide (**1-rGO**). The heterogeneous catalyst originates an increasing in the reaction rate and the yield into the product.

[a] P. Ballestín, Dr. A. Caballero, Prof. Dr. P. J. Pérez
Laboratorio de Catálisis Homogénea, Unidad Asociada al CSIC
CIQSO-Centro de Investigación en Química Sostenible and Departamento de Química
Universidad de Huelva, 21007-Huelva (Spain)
Fax: (+34)959219942
E-mail: perez@dqcm.uhu.es; ana.caballero@dqcm.uhu.es

[b] D. Ventura-Espinosa, Dr. J. A. Mata
Institute of Advanced Materials (INAM),Universitat Jaume I, Avda. Sos Baynat s/n, 12006 Castellón, Spain
E-mail: jmata@qio.uji.es;

[c] Dr. S. Martín
Dept. de Química Física, Facultad de Ciencias, Instituto de Ciencias de Materiales de Aragón (ICMA), Universidad de Zaragoza-CSIC, 50009 Zaragoza (Spain)

The ORCID identification number(s) for the authors of this article can be found under https://doi.org/10.1002/chem.2018XXXXXt.

graphene surface.[8] It has been recently disclosed that the substituent on the pyrene fragment affect the conductivity of the graphene material.[9] We reasoned that with a relatively close metal center, such electronic flux could affect the performance of the former during catalysis, particularly in this transformation where an electrophilic metallocarbene is involved. [10] In fact, one of our groups has previously employed this fixation methodology but for the gold-catalyzed intramolecular hydroamination of alkynes.[11] In this contribution, we describe a new copper complex bearing an NHC ligand bearing a pyrene tail at the backbone (Scheme 1) that can be adsorbed onto reduced graphene oxide (rGO), as well as their use as catalysts for carbene transfer reactions to alkanes and benzene. Interestingly, we have observed the increase of both the reaction rate and the yields toward hydrocarbon functionalization with the supported catalyst, features that we explain as the result of an electronic effect on the metal center generated at the remote pyrene-rGO interaction.

Results and discussion

Synthesis of the discrete and supported copper complexes.

We first targeted the synthesis of the imidazolium salt of the NHC-modified ligand L^{Mes} (Scheme 2) bearing mesityl groups at the N atoms and an O-CH_2-pyrenyl fragment at the backbone. Toward that end, we employed the strategy previously described by Cesar and co-workers, [12] upon reaction of bromomethylpyrene with the corresponding 4-hydroxylimidazolium salt, leading to the isolation of L^{Mes}Br in 71% yield. L^{Mes}Br was straightforwardly characterized from their NMR spectra and analytical data (see Experimental Section).

The copper(I) complex bearing L^{Mes} was prepared upon deprotonation of L^{Mes}Br in the presence of potassium carbonate, leading to the isolation of L^{Mes}CuBr (**1**) in 74% (Scheme 2). Complex **1** was characterized by NMR and elemental analysis. Spectroscopic data is in agreement with the existence of an NHC ligand coordinated to copper as inferred from the observance of a resonance at 174.4 ppm in the $^{13}C\{^1H\}$ NMR spectrum.

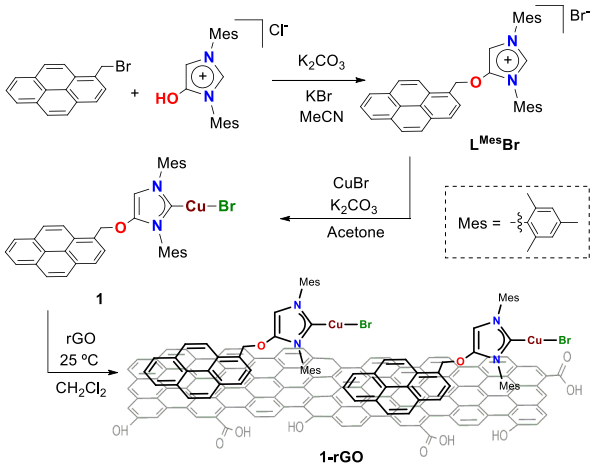

Scheme 2. Synthetic route for the preparation of L^{Mes}Br, L^{Mes}CuBr (**1**) and L^{Mes}CuBr-rGO (**1-rGO**).

As mentioned above, the presence of the pyrene moiety in the L^{Mes} ligand is very convenient toward its adsorption onto graphenic surfaces.[13] We have now performed the immobilization of complex **1** onto the surface of reduced graphene oxide (rGO) at room temperature by impregnation of a rGO suspension with a dichloromethane solution of complex **1** (Scheme 2). After 24 h of stirring at room temperature, the solid was filtered off, washed and dried. The use of mild conditions ensures that the properties of the molecular complex and the rGO are preserved during the immobilization step. The hybrid material **1-rGO** has been characterized by different techniques such as HRTEM, XPS, UV/vis and ICP/MS (see SI for full details). Determination of the exact amount of copper on the surface of graphene is crucial toward further catalytic uses: ICP/MS analysis of **1-rGO** reported an amount of 8.0 wt% of complex **1** onto the graphene.

A comparative analysis of complex **1** and **1-rGO** was performed by X-ray photoelectron spectroscopy (XPS). The

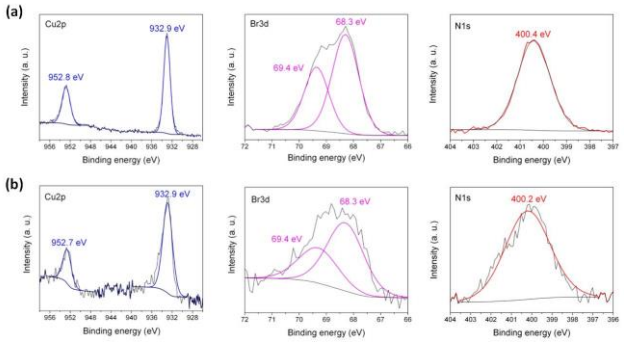

Figure 1. Comparative XPS analysis of the core-level peak of N1s, Br3d and Cu2p for the complex **1** (top) and the hybrid material **1-rGO** (bottom).

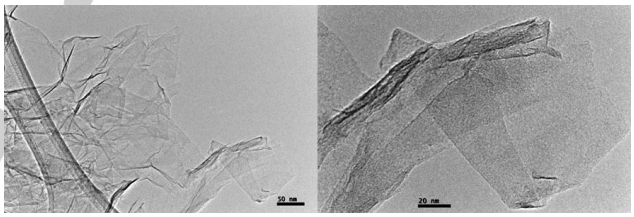

Figure 2. HRTEM images of **1-rGO** at different magnifications.

results for **1-rGO** show the characteristic core-level peaks of Cu 2p, Br 3d and N 1s at the same binding energy of complex **1** (Figure 1). The binding energy of Cu 2p confirms the +1 oxidation state in both complex **1** and **1-rGO**. The XPS analysis suggests the immobilization of complex **1** onto the surface of graphene without alteration in its structure or oxidation state. Additional HRTEM studies of hybrid material **1-rGO** shows that graphene maintains the same morphology after the immobilization process (Figure 2). Also, the energy-dispersive X-ray spectroscopy (EDX) elemental analysis shows the presence of copper homogeneously distributed on the surface of graphene. UV/Vis measurement of a suspension of **1-rGO** shows the presence of the characteristic bands of the pyrene tag, confirming that complex **1** is immobilized onto the graphene (Figure S7). All data collected from those characterization techniques assess that the

nature of complex **1** and the properties of the support are preserved during the immobilization process. Thus, the solid **1-rGO** seems appropriate to compare its potential catalytic activity with that of the soluble, discrete complex **1** and to evaluate the differences due to the graphene support.

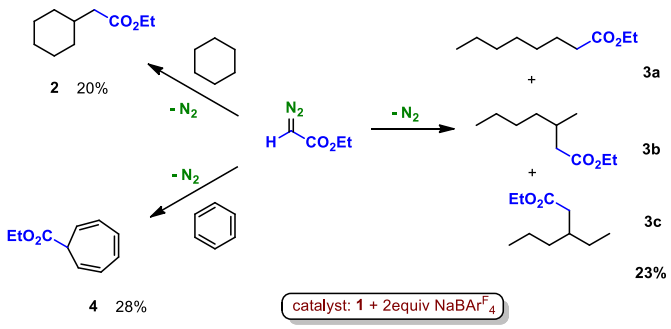

Scheme 3. Catalytic activity of complex **1** toward carbene transfer to cyclohexane, hexane and benzene.

Catalytic activity of 1 and 1-rGO toward hydrocarbon functionalization with ethyl diazoacetate.

We have chosen three hydrocarbons as model substrates to test the capabilities of these copper-based materials toward the catalytic transfer of the carbene $CHCO_2Et$ group from ethyl diazoacetate (EDA). Cyclohexane, n-hexane and benzene were reacted with EDA in the presence of catalytic amounts of **1**, using 2 equiv of $NaBAr^F_4$, with respect to the catalyst as halide scavenger. The experiments led to the incorporation (Scheme 3) of such carbene group to cyclohexane (**2**) or hexane (**3a-c**), upon copper-mediated insertion into the C-H bonds,[4] or the addition to the double bond of benzene, affording a cycloheptatriene (**4**) in the so-called Buchner reaction.[14] Albeit yields were lower than those previously reported for related NHCCuCl catalysts,[15] these values are large enough for comparative purposes with those of the heterogeneized version of **1** (vide infra). It is worth noting that EDA was not completely consumed after 21 h of stirring, and that the products derived from catalytic carbene coupling, i. e. diethyl fumarate and maleate accounted for a small fraction of initial EDA. [16]

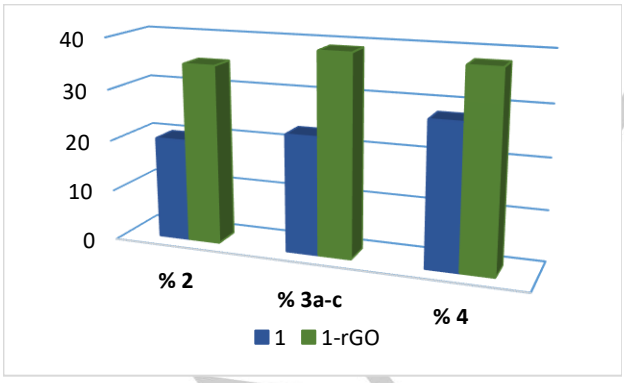

Figure 3. Comparison of the catalytic activity of **1** and **1-rGO** for the reactions shown in Scheme 3.

Once the moderate catalytic activity of **1** was assessed, we moved toward its supported version, **1-rGO**. Under identical conditions of temperature, copper and EDA loadings and reaction time, the three hydrocarbons shown in Scheme 3 were employed as substrates with **1-rGO** as the catalyst (with 2 equiv of $NaBAr^F_4$ as halide scavenger). Figure 3 displays the comparison of yields of both homo- and heterogeneous catalytic systems, an increase being observed with the latter: 15% in **2**, 16% in **3a-c** and 10% in **4**. Again, EDA was not fully consumed, even after 4 days of stirring at room temperature. HRTEM images of the **1-rGO** materials after catalysis revealed that the structure seems unaltered, without the formation of aggregates or metal nanoparticles (see Figure S10).

Intrigued by the lack of complete consumption of EDA, we carried out experiments measuring the evolution of N_2 with time (Figure 4). First, the well-known, very active $Tp^{Br3}Cu(NCMe)$ catalyst[17] for cyclohexane functionalization with EDA was employed, providing the exact amount of N_2 that should be released with the initial amount of EDA (0.25 mmol). Then, under the same conditions, **1** and **1-rGO** were employed as catalysts in separate experiments. As shown in Figure 4, both catalysts induced the exponential growth typically observed for N_2 formation in these transformations.[18] However, the amount of evolved gas did not reach the expected limit of 0.25 mmol, marked by the experiment with the $Tp^{Br3}Cu(NCMe)$ catalyst, but stopped at ca. 60% of such amount (0.15-0.16 mmol) with both the homogeneous and the heterogeneous catalysts, in line with the observation of some unreacted EDA at the end of the catalytic transformations shown in Scheme 3. The fact that the amount of nitrogen evolved is nearly the same with **1** and **1-rGO** points

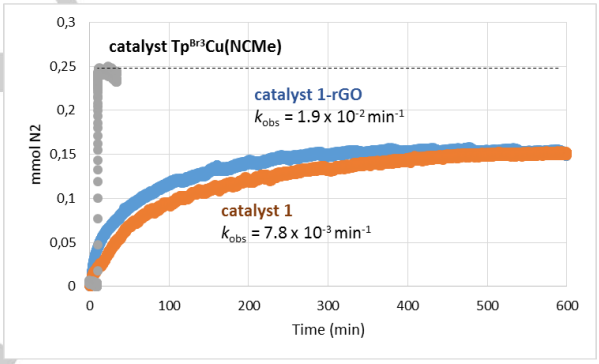

Figure 4. Kinetic curves for the evolution of N_2 in the reaction of cyclohexane and EDA at room temperature. The grey curve corresponds to $Tp^{Br3}Cu(NCMe)$ as the catalyst, providing the expected maximum amount of evolved N_2.

toward a deactivation process affecting the metal center in a similar manner.

To evaluate the reversibility of this catalytic inhibition, catalyst recycling was performed with heterogeneous **1-rGO** by simply filtering off the reaction mixture and reusing the solid residue (see Experimental). As a representative example we employed n-hexane as the substrate. Figure 5 displays the results of three consecutive runs, showing that the catalyst remains active, in spite of not consuming all the EDA at the end of each cycle. We believe that the inhibition process along the catalytic reaction, can be reversed at the end of the cycle when the reaction is filtered and the solid washed before use. The observed decrease in yields across the cycles should be due to the loss of a portion of the solid catalyst during workup. It is also worth mentioning that the filtrate obtained at the end of each cycle was not active

toward additional EDA, indicating the absence of substantial catalyst leaching. At this stage, we do not have an explanation for the inhibition of the catalyst avoiding the complete consumption of EDA.

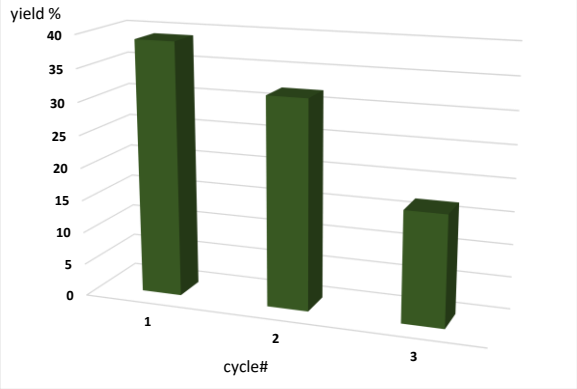

Figure 5. Catalyst recycling for n-hexane (left). Yields are referred to initial EDA.

A second feature observed from the kinetic experiments is that the reaction rate constant for nitrogen evolution (that is the same for EDA consumption, since one molecule of EDA generates one molecule of N_2) with heterogeneous catalyst is higher than that for the homogeneous counterpart: k_{obs}(**1-rGO**) = 1.9 x 10^{-2} min^{-1} vs k_{obs}(**1**) = 7.8 x 10^{-3} min^{-1} (Figure 4). It is well established that N_2 evolution in these transformations is the rate determining step leading to the formation of a metallocarbene intermediate, and that the rate is faster for more electrophilic metal centers.[10,19] Additionally, it is also known that the higher the electrophilicity at the metal-carbene intermediate, the higher the yields into the C-H functionalization products.[10] With these two ideas in mind, it seems reasonable assuming that the copper center at **1-rGO** is more electrophilic than that in **1**, explaining the observed behavior in yields and reaction rates. In other words, the catalytic activity of **1** is enhanced when supported on rGO, this adsorption generating a decrease in the electron density at

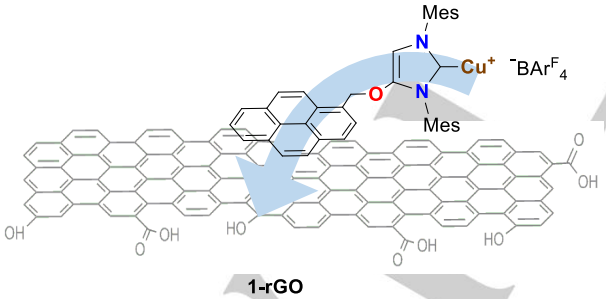

Scheme 4. Electronic flux in **1-rGO** accounting for the experimentally observed enhanced reaction rate and yields. The red arrow shows the electronic flux that originate a net decrease in electronic density at the copper center.

the metal center. This proposal finds support in a recent contribution by Lee and co-workers,[9] which demonstrated that the substituents at the pyrene ring infer a variation in the conductivity at graphene due to electron transfer from or to pyrene. In our case, the –CH_2-O-NHC substituent must act as an electron-donating group, increasing electron density at graphene with the corresponding decrease at the copper complex (Scheme 4). This remote pyrene-graphene stacking effect explains the enhancement of reaction rate and yields observed with **1-rGO** when compared with those of soluble **1**.

Conclusions

The copper complex bearing a NHC ligand with a pyrene tag attached to the ligand backbone has been synthetized, fully characterized and supported onto reduced graphene oxide. Both the soluble complex **1** and the anchored derivative **1-rGO** have been employed as catalysts for the functionalization of hexane, cyclohexane or benzene in transformations involving the incorporation of the carbene unit $CHCO_2Et$ to the hydrocarbon molecule. The catalytic activity of the heterogeneous catalyst **1-rGO** displays higher reaction rate as well as an enhancement of the yields into the functionalized products, thus the anchored complex being more effective than the homogeneous counterpart. This behavior must be related to an increase of electrophilicity at the metal center due to an electronic flux from the copper complex to the graphene surface through the pyrene tag.

Experimental Section

General. All reactions were carried out under an oxygen free nitrogen atmosphere by using an MBraun-Unilab glovebox containing dry argon or nitrogen or conventional Schlenk techniques. Anhydrous solvents were dried using a solvent purification system (SPS). EDA, $NaBAr^F_4$ and hydrocarbons for catalytic experiments were purchased from Sigma-Aldrich and used without previous purification. Nuclear magnetic resonance (NMR) spectra were recorded at room temperature with the appropriate deuterated solvent on Bruker spectrometers operating at 300 or 400 MHz (^{1}H NMR), and referenced to $SiMe_4$. Elemental analysis were carried out in a TruSpec Micro Series. Electrospray Mass Spectra (ESI-MS) were recorded on a MicroMass Quatro LC instrument. Methanol was used as mobile phase and nitrogen was used as the drying and nebulizing gas. High-resolution images of transmission electron microscopy (HRTEM) and high-angle annular dark-field. X-ray photoelectron spectra (XPS) were acquired on a Kratos AXIS ultra DLD spectrometer with a monochromatic Al Kα X-ray source (1486.6 eV) using a pass energy of 20 eV. To provide a precise energy calibration, the XPS binding energies were referenced to the C1s peak at 284.6 eV. UV-vis spectra were acquired on a Varian Cary 50 spectrophotometer. GC studies were ferformed on a Bruker GC-450 gas chromatography instrument with a FID detector using 30 m x 0.25 mm CP-Sil 8CB capillary column (catalytic reactions).

Synthesis of L^{Mes}Br. 4-hydroxy-1,3-dimesitylimidazolium chloride (600 mg, 1.68 mmol) was suspended in 40 mL of dry acetonitrile. Potassium carbonate (470.6 mg, 3.4 mmol) and potassium bromide (614 mg, 5.1 mmol) were added and the mixture was stirred at room temperature for 1 h. Then bromomethyl pyrene (516 mg, 1.74 mmol) was added and the mixture was stirred at 60 ºC for 18 hours. The solvent was removed, dichloromethane (35 mL) was added and the mixture was filtered through a pad of celite to remove the insoluble inorganic salts. The solvent was evaporated and the product was

recrystallized using a mixture (1:1) of acetone/pentane. The imidazolium salt **L^{Mes}Br** was obtained as a pale yellow powder. Yield: 740 mg (71 %). ^{1}H NMR (300 MHz, CD_3OD) δ 8.89 (d, *J* = 1.7 Hz, 1H, NC*H*N), 8.26 (d, *J* = 7.2 Hz, 2H, CH_{pyr}), 8.23 – 7.89 (m, 7H, CH_{pyr}), 7.81 (d, *J* = 1.7 Hz, 1H, CH_{imid}), 7.15 (s, 2H, CH_{Mes}), 6.74 (s, 2H, CH_{Mes}), 6.04 (s, 2H, CH_2), 2.37 (s, 3H, CH_{3Mes}), 2.20 (s, 3H, CH_{3Mes}), 2.10 (s, 6H, CH_{3Mes}), 1.61 (s, 6H, CH_{3Mes}). ^{13}C{^{1}H} NMR (75 MHz, CD_3OD) δ [148.2, 142.9, 142.8, 136.1, 135.6, 134.2] (*C*$_{pyr}$, *C*H$_{Mes}$), 133.7 (NCHN), [132.8, 132.5, 132.0, 131.3, 130.8, 130.4, 130.0] (*C*$_{pyr}$, *C*H$_{Mes}$, *C*$_{imid}$), [129.6, 129.5] (*C*H$_{Mes}$) [128.3, 128.2, 127.8, 127.6, 127.1, 127.0, 126.1, 125.4, 125.3, 123.7] (*C*$_{pyr}$, *C*H$_{Mes}$, *C*$_{imid}$), 106.7 (*C*H$_{imid}$), 76.3 (*C*H$_2$), [21.1, 21.1, 17.2, 17.2] (*C*H$_{3Mes}$). Electrospray MS (Cone 20 V) (m/z, fragment): 535.2 [M-Br]$^+$. Anal. Calculated for $C_{38}H_{35}BrN_2O$: C, 74.1; H, 5.7; N, 4.5 Found: C 74.0, H 5.4, N, 4.4.

Synthesis of complex 1. In a pyrex tube, imidazolium salt (**L^{Mes}Br**) (575mg, 0.93 mmol), CuBr (134.8 mg, 0.93 mmol), K_2CO_3 (767.7 mg, 5.58 mmol) and 5 mL of acetone were heated at 60 ºC for 18 h. Then, the solvent was removed under vacuum, dichloromethane was added (10 mL) and the mixture was filtered through silica. The pad of silica was washed with dichloromethane (10 mL). The solvent was reduced to approximately 2 mL and pentane was added, affording a pale yellow solid, which was filtered off and dried in vacuum. Yield: 480 mg (76%). ^{1}H NMR (300 MHz, $CDCl_3$) δ 8.23 (d, *J* = 7.6 Hz, 2H, CH_{pyr}), 8.14 – 7.98 (m, 6H, CH_{pyr}), 7.87 (d, *J* = 7.6 Hz, 1H, CH_{pyr}), 6.93 (s, 2H, CH_{Mes}), 6.93 (s, 2H, CH_{Mes}), 6.37 (s, 1H, CH_{imid}), 5.66 (s, 2H, CH_2), 2.31 (s, 3H, CH_{3Mes}), 2.29 (s, 3H, CH_{3Mes}), 2.04 (s, 6H, CH_{3Mes}), 1,97 (s, 6H, CH_{3Mes}). ^{13}C{^{1}H} NMR (75 MHz, CDCl3) δ 174.4 (*C*$_{carbene\text{-}Cu}$), [146.9, 139.1, 139.0, 135.4, 134.9, 134.4, 132.0, 131.0, 130.8, 130.3, 129.3, 129.1, 129.0, 128.1, 128.0, 127.1, 126.9, 126.7, 126.1, 125.6, 125.5, 124.6, 124.1, 123.9, 122.1, 100.9] (*C*$_{pyr}$, *C*H$_{Mes}$, *C*$_{imid}$), 73.5 (*C*H$_2$), [20.8, 20.8, 17.6, 17.3] (*C*H$_{3Mes}$)]. Anal. Calcd. for $C_{38}H_{35}BrN_2O$: C, 67.3; H, 5.0; N, 4.1. Found: C, 67.1, H 5.4, N 4.4.

Synthesis of 1-rGO. A suspension of 315 mg of reduced graphene oxide in 10 mL of CH_2Cl_2 was inmersed in an ultrasound bath for 30 min. Then, 70 mg of **1** were added to the mixture. The suspension was stirred at room temperature for 24 h. The black solid was isolated by filtration and washed with 200 mL of CH_2Cl_2 affording the hybrid material as a black solid. The exact amount of supported complex was determined by ICP-MS analysis. The results accounted for a 8 wt% of complex **1** in the hybrid material **1-rGO**, that was characterized by UV/Vis, XPS and HRTEM.

Catalytic experiments with complex 1. In a Schlenk flask, complex **1** (0.01 mmol, 7 mg) was dissolved in the hydrocarbon (cyclohexane, hexane, or benzene; 15 mL) and 2 eq. of $NaBAr^F_4$ (17.8 mg) were added as halide scavenger. The mixture was stirred for 15 min. A solution of EDA (1 mmol, 124.56 µL) in the hydrocarbon (5 mL) was then added over 21 h with the aid of a syringe pump. In the case of cyclohexane and hexane, the yields were determined by GC analysis by using calibration curves. In the case of benzene, the yields were determined by NMR analysis by using internal standard (see Supporting Information for more details).

Catalytic experiments with complex 1-rGO. Following the previous procedure, complex **1-rGO** (0.005 mmol, 21 mg) was dissolved in the hydrocarbon (cyclohexane, hexane, or benzene; 15 mL) and 2 eq. of $NaBAr^F_4$ (17.8 mg) were added. A solution of EDA (0.5 mmol, 62.28 µL) in the alkane (5 mL) was then added over 21 h with the aid of a syringe pump. Once finished, the solid catalyst was filtered off, washed with 3 x 10 mL of the corresponding hydrocarbon and dried under vacuum. The collected filtrates were investigated using the same protocols mentioned above (see Supporting Information for full description). The second run was set up upon adding fresh hydrocarbon, halide scavaneger and the solution of EDA in the corresponding substrate, this procedure being repeated for several cycles.

Kinetic experiments on dinitrogen evolution. Catalyst **1** or **1-rGO** (0.0025 mmol) was dissolved/suspended in cyclohexane (5 mL) in a Man on the Moon© apparatus (see Supporting Information) capable of measuring pressure variation. After 15 minutes of stirring for pressure stabilization, 0.005 mmol of $NaBAr^F_4$ was added. Then, 100 equivalent of EDA (0.25 mmol, 31.14 µL) were added in one portion and the mixture was stirred at room temperature. The nitrogen evolution was measured until the pressure remained constant.

Acknowledgements

The authors would like to thank the financial support of the MINECO (CTQ2017-82893-C2-1-R and CTQ2015-69153-C2-2-R), Junta de Andalucía (P12-FQM-1765) and Universitat Jaume I (UJI-B2018-23). D. V-E thanks the MINECO for a grant (FPU15/03011). The authors thank the 'Servei Central d'Instrumentació Científica (SCIC)' of the Universitat Jaume I.

Conflict of interest

The authors declare no conflict of interest.

Keywords: alkane C-H functionalization • carbene transfer • graphene supported catalysts • pyrene graphene interaction • catalyst anchoring

[1] *Homogeneous Catalysis, Understanding the Art*. P. W. N. M van Leeuwen. Kluwer Academic Publishers, Dordrecht, 2004.

[2] D. J. Cole-Hamilton. *Science* **2003**, *299*, 1702 – 1706.

[3] R. Augustine, S. Tanielyan, S. Anderson, Y. Gao, P. Goel, N. Mahata, J. Nair, C. Reyes, H. Yang, A. Zsigmond in *Methodologies in Asymmetric Catalysis*, ACS Symposium Series, Vol. 880, chapter 2 *Anchored Homogeneous Catalysts: The Best of Both Worlds*, 2004.

[4] A. Caballero, M. M. Díaz-Requejo, M. R. Fructos, A. Olmos, J. Urbano, P. J. Pérez. *Dalton Trans.* **2015**, 44, 20295-20307.

[5] A. Caballero, E. Despagnet-Ayoub, M. M. Díaz-Requejo, A. Díaz-Rodríguez, M. E. González-Núñez, R. Mello, B. K. Muñoz, B. K.; W. Solo-Ojo, G. Asensio, M. Etienne, P. J. Pérez *Science,* **2011**, *332*, 835-838

[6] M. A. Fuentes, B. K. Muñoz, K. Jacob, L. Vendier, A. Caballero, M. Etienne, P. J. Pérez, *Chem. – Eur. J.*, **2013**, *19*, 1327-1334.

[7] J. T. Sarmiento, A. Olmos, T. R. Belderrain, A. Caballero, T. Varea, P. J. Pérez, G. Asensio. *ACS Sustainable Chem. Eng*. 2019, 10.1021/acssuschemeng.9b00523.

[8] a) B. F. Machado, P. Serp. *Catal Sci. Technol.* **2012**, *2*, 54-75. V. Georgakilas, M. Otyepka, A. B. Bourlinos, V. Chandra, N. Kim, K. C. Kemp, P. Hobza, R. Zboril, K. S. Kim. *Chem. Rev.* **2012**, *112*, 6156-6214.

[9] J. Lee, E. Hwang, E. Lee, S. Seo, H. Lee. *Chem. Eur. J.* **2012**, *18*, 5155-5159.

[10] A. Caballero, P. J. Pérez, *J. Organomet. Chem*. **2015**, *793*, 108-113.

[11] D. Ventura-Espinosa, S. Sabater, J. A. Mata. *J. Catal*. **2017**, *352*, 498-504.

[12] L. Benhamou, V. César, H. Gornitzka, N. Lugan, G. Lavigne. *Chem. Commun.* **2009**, 4720–4722.
[13] a) D. Ventura-Espinosa, C. Vicent, M. Baya, J. A. Mata. *Catal. Sci. Technol.* **2016**, *6*, 8024–8035; b) D. Ventura-Espinosa, A. Carretero-Cerdán, M. Baya, H. García, J. A. Mata. *Chem. Eur. J.* **2017**, *23*, 10815–10821; c) D. Ventura-Espinosa, S. Sabater, A. Carretero-Cerdán, M. Baya, J. A. Mata. *ACS Catal.* **2018**, *8*, 2558–2566.
[14] E. Buchner, T. Curtius, *Ber. Dtsch. Chem. Ges*. **1885**, *18*, 2371-2377.
[15] M. R. Fructos, M. Besora, A. A. C Braga, M. M. Díaz-Requejo, F. Maseras, P. J. Pérez. *Organometallics* **2017**, *36*, 172-179.
[16] I. Rivilla, W. M. C. Sameera, E. Álvarez, M. M. Díaz-Requejo, F. Maseras, P. J. Pérez. *Dalton Trans.* **2013**, *42*, 4132-4138.
[17] A. Caballero, M. M. Díaz-Requejo, T. R. Belderrain, M. C. Nicasio, S. Trofimenko and P. J. Pérez, *J. Am. Chem. Soc*., **2003**, *125*, 1446-1447.
[18] See for example: A. Pereira, Y. Champouret, C. Martín, E. Álvarez, M. Etienne, T. R. Belderraín, P. J. Pérez, *Chem. – Eur. J*., **2015**, *21*, 9769-9775.
[19] A. Olmos, R. Gava, B. Noverges, D. Bellezza, K. Jacob, M. Besora, W. M. C. Sameera, M. Etienne, F. Maseras, G. Asensio, Ana Caballero, P. J. Pérez. *Angew. Chem. Int. Ed*. **2018**, *57*, 13848-13852.

Received: ((will be filled in by the editorial staff))
Revised: ((will be filled in by the editorial staff))
Published online: ((will be filled in by the editorial staff))

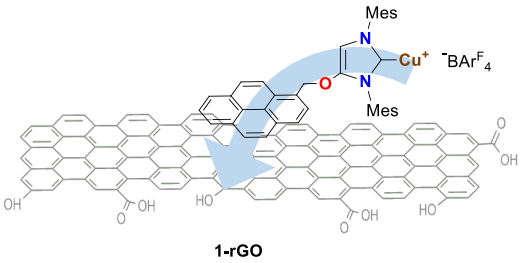

1-rGO

Anchoring a NHC-Cu(I) complex onto graphene through a pyrene antenna induces the enhancement of the catalytic properties of the copper center toward hydrocarbon functionalization by carbene transfer from ethyl diazoacetate

Remote Catalyst Tuning

Pilar Ballestin, David Ventura-Espinosa, Santiago Martín Ana Caballero, Jose A. Mata* and Pedro J. Pérez**

■■ – ■■

Improving Catalyst Activity in Hydrocarbon Functionalization by Remote Pyrene-Graphene Stacking